INTERNATIONAL SOCIETY FOR SOIL MECHANICS AND GEOTECHNICAL ENGINEERING



This paper was downloaded from the Online Library of the International Society for Soil Mechanics and Geotechnical Engineering (ISSMGE). The library is available here:

https://www.issmge.org/publications/online-library

This is an open-access database that archives thousands of papers published under the Auspices of the ISSMGE and maintained by the Innovation and Development Committee of ISSMGE.

The paper was published in the proceedings of the 20th International Conference on Soil Mechanics and Geotechnical Engineering and was edited by Mizanur Rahman and Mark Jaksa. The conference was held from May 1st to May 5th 2022 in Sydney, Australia.

Mechanically stabilized earth wall monitoring technique based on image processing gathered from single view of camera

Technique de surveillance des murs en terre stabilisée mécaniquement basée sur le traitement d'images recueillies à partir d'une vue unique de la caméra

Yong Soo Ha and Yun Tae Kim

Dept. of Ocean Engineering, Pukyong national University, Busan, Republic of Korea, hok3662@naver.com

ABSTRACT: Mechanically stabilized earth wall (MSEW) is widely used to expand construction areas and overcome the limitations of fields. Nowadays, a lot of retaining walls have still collapsed due to the difficulty of real-time monitoring of MSEW, which attributes to time and budget problems. This study suggests a monitoring technique using single camera system to detect the displacement of MSEW blocks through a vision based images. In the retaining wall system, most deformations come from facing displacements and settlements. Through these assumptions, this study overcomes the limitation of using two or more cameras to determine three-dimensional displacement measurement. In this study, 2 steps of experiments were conducted to validate the single camera system. 1) The optical feature matching technique was selected block behavior detection experiment for the ability to detect the same block before and after the behavior, and 2) structure displacement measuring capability with three different displacement types was also verified through the structure behavior detection experiment. The results show that errors were within 3.34%. As a result, the proposed single camera system using image processing can be widely used to inspect and monitor the stability of MSEW.

RÉSUMÉ: Le mur en terre stabilisée mécaniquement (MSEW) est largement utilisé pour étendre les zones de construction et surmonter les limites des champs. De nos jours, de nombreux murs de soutènement se sont encore effondrés en raison de la difficulté de surveiller en temps réel le MSEW, ce qui attribue des problèmes de temps et de budget. Cette étude suggère une technique de surveillance utilisant un système de caméra unique pour détecter le déplacement des blocs MSEW à travers des images basées sur la vision. Dans le système de mur de soutènement, la plupart des déformations proviennent de déplacements et de tassements de parement. Grâce à ces hypothèses, cette étude surmonte la limitation de l'utilisation de deux caméras ou plus pour déterminer la mesure du déplacement en trois dimensions. Dans cette étude, 2 étapes d'expériences ont été menées pour valider le système à caméra unique. 1) La technique d'appariement des caractéristiques optiques a été sélectionnée pour l'expérience de détection du comportement du bloc pour la capacité de détecter le même bloc avant et après le comportement, et 2) la capacité de mesure du déplacement de la structure avec trois types de déplacement différents a également été vérifiée grâce à l'expérience de détection du comportement de la structure. Les résultats montrent que les erreurs étaient inférieures à 3.34 %. En conséquence, le système de caméra unique proposé utilisant le traitement d'images peut être largement utilisé pour inspecter et surveiller la stabilité du MSEW.

KEYWORDS: Image processing; feature detector; feature descriptor; single camera system; structure health monitoring.

1 INTRODUCTION.

With the development of image processing technology, visionbased analysis technology is being applied in various fields such as image-based structure health monitoring, biomedical imaging, and remote sensing. In particular, feature detection and descriptors are widely used that extract features of an image and match a specific target image to find a problem, or perform registration through the matched features to match the image into one. Various studies have been conducted to measure the behavior of the bridge, soil nail wall, retaining wall model, and slope by using three-dimensional coordinates based on registration of images taken from two or more points of view (Jiang and Jauregui 2010; Esmaeili et al. 2013; Oats et al. 2017; Zhao et al. 2018). In order to analyze in real time a stereo camera system that analyzes an object based on images taken from two or more viewpoints as described above, there is an economic disadvantage that two or more cameras must be installed. In addition, if one camera shoots in stages from multiple viewpoints, monitoring cannot be performed in real time.

The structural behavior analysis technology using a vision based image analyzed the behavior in the xy axis for an object perpendicular to the camera (Lee and Shinozuka 2006; Choi et al. 2011; Fukuda et al. 2013; Feng et al. 2015). However, since it analyzes the vertical and horizontal behavior of the target structure perpendicular to the camera, the behavior occurring in the forward direction of the structure cannot be analyzed.

In general, the depth image (the distance between the object and the camera) is essential to extract and analyze 3D coordinates using the image. Therefore, a depth image may be constructed by utilizing images captured from two or more camera viewpoints or directly measuring through optical equipment such as RaDAR and LiDAR. Researches that construct 3D point clouds of various structures using laser scanner, mobile LiDAR mapping system (MLS), and LiDAR to measure displacement and behavior are being actively developed in the field of 3D measurement (Oskouie et al. 2016; Aldosari et al. al., 2020). However, these remote sensing devices and software are expensive. In addition, for the same reason as the stereo camera system, in order to monitor in real time, it is more expensive because shooting must be performed at various points in time.

In this study, a vision based MSEW monitoring technology was developed to perform real-time inspection and monitoring. It was defined as a single camera system in a form similar to a stereo camera system because it uses an image from a single viewpoint. In general, due to the continuous shape of the retaining wall in the lateral direction, collapse occurs mainly due to forward displacement and settlement. Various studies were conducted to evaluate the stability of the retaining wall according to changes in various collapse parameters such as reinforcement, surface load, and consolidation period (Yang et al. 2009; Leonards et al. 1994; Koseki and Hayano 2000; Shinde and Mandal 2007; Bathurst and Benjamin 1990; Benjamim et al., 2007; Panah et al. 2015). To evaluate the stability of the retaining wall, the forward displacement and settlement were mainly measured, and the effects of various collapse inducing factors or

the effect of reinforcement and stability improvement were analyzed.

Therefore, the behavior of the reinforced soil retaining wall that occurs mainly is divided into horizontal displacement in the facing direction and vertical displacement represented by settlement. fig. 1 shows an example of behavior in images when structure behavior occurs in single camera system. In the image taken from a position parallel to the ground surface and inclined by θ_x to the structure, the amount of x change is analyzed as a horizontal displacement in the anteroposterior direction, and the amount of y change is analyzed as a vertical displacement perpendicular to the surface. Therefore, the three-dimensional behavior of the reinforced soil retaining wall is measured without applying techniques for extracting the depth image.

A feature matching technique was applied to extract the same front part of the reinforced soil retaining wall. Matching performance was evaluated by generating horizontal displacement (facing displacement), vertical displacement (settlement), and combined displacement for one reinforced soil retaining wall block. The optimal feature matching technique was used to analyze the behavior of structures in the form of reinforced soil retaining walls made by stacking blocks. The performance evaluation of the reinforced soil retaining wall behavior of the single camera system was evaluated by comparing the measured value using the total station and the calculated value using the single camera system.

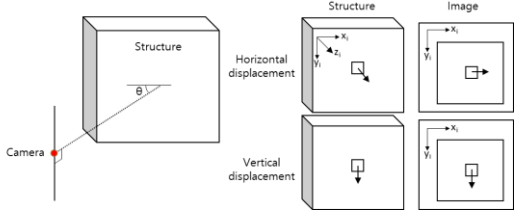


Figure 1. Example of behavior in images when structure behavior occurs in single camera system.

2 METHOD

2.1 Feature matching

Feature matching extracts features from image pairs and matches the same features among them to perform image registration. Feature matching shows various performances according to changes in target, scale, and rotation depending on the detector and descriptor used. Therefore, it is necessary to select a technique that shows the optimal performance according to the change in the behavior in the three-dimensional space for the reinforced soil retaining wall block.

Performance evaluation was performed for three techniques such as KAZE, SURF, and MinEigen, and the optimal feature detector and descriptor for the MSEW type retaining wall was evaluated through the performance evaluation. Feature matching performance was evaluated based on repeatability based on the number of matched features and BRE (Block registration error) based on the location error in the matched features. Fig. 2 shows example of features and vertices to determine repeatability and BRE, and the equations for calculating each indicator are shown below (Eq. 1 and Eq. 2).

$$Repeatability = \frac{N_m}{N_{di}} \tag{1}$$

Where N_m is the number of matching points in image pairs and N_{di} is the number of detected points in target image at initial state (In case of figure 1, repeatability is 5/5 = 1).

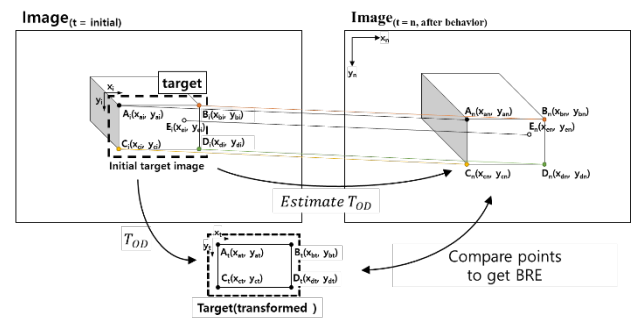


Figure 2. Example of features and vertices to determine repeatability and BRE.

$$BRE_{h1} = |A_t - B_t| - |A_n - B_n|$$

$$BRE_{v1} = |A_t - C_t| - |A_n - C_n|$$

$$BRE_{h2} = |C_t - D_t| - |C_n - D_n|$$

$$BRE_{v2} = |B_t - D_t| - |B_n - D_n|$$

$$BRE = \frac{BRE_{h1} + BRE_{v1} + BRE_{h2} + BRE_{v2}}{A}$$
(2)

Where BRE_{h1} , BRE_{h2} are the up and down side of block registration error in horizontal axis, and BRE_{v1} , BRE_{v2} are the the left and right side of block registration error in vertical axis, respectively. A_n , B_n , C_n , D_n = location of the top left, top right, bottom left, bottom right vertex of the block after displacement occurs(t=n), respectively. A_t , B_t , C_t , D_t = The position of the top left, top right, bottom left, bottom right vertex of the block in the transformed target, respectively.

2.2 Single camera system

Fig. 3 shows that the horizontal and vertical behavior of the MSEW in a single camera system was calculated as Δd_{xi} and Δd_{yi} in the image captured at a single viewpoint. In the image taken from a position parallel to the ground surface and inclined by θ_x , the amount of Δd_{xi} change was analyzed as a horizontal displacement in the front-to-back direction, and the amount of Δd_{yi} change was analyzed as a vertical displacement perpendicular to the ground surface.

In the single camera system, feature matching is performed to extract the same block as a target, and Δd_{xi} and Δd_{yi} are obtained by comparing images before and after the behavior of the same block. After that, the actual horizontal and vertical displacement of the structure is calculated by applying Δd_{xi} and Δd_{yi} to the equation developed using the distance between the camera and the structure (D_r), the angle in the x direction of the camera and the structure (θ_x) and camera parameters.

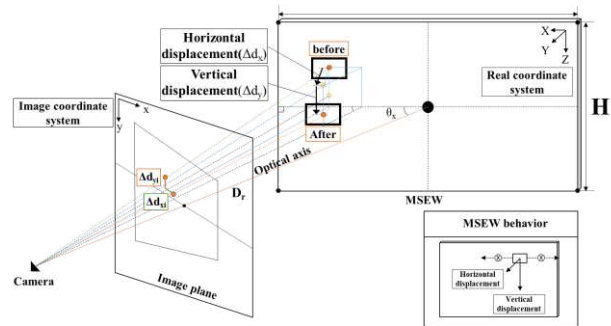


Figure 3. Schematic diagram of displacement calculation module in single camera system

3 LABORATORY EXPERIMENT

3.1 Block behavior detection experiment

Fig. 4 shows the X, Y, Z linear stage and example of block behavior detection experiment. horizontal displacement (10mm), Vertical displacement(-10mm), and combined displacement (10mm, -10mm) were described by using X, Y, Z linear stage. The feature matching performance was evaluated for three types of behavioral images, and feature matching was performed by



applying three feature detectors and descriptors to images before and after behavior. In order to select the optimal detector and descriptor that shows the best performance in various θ_x and behavior types, experiments were performed on $12~\theta_x$ distributed in $5\sim85^{\circ}$. The block behavior detection performance of the single camera system was evaluated by comparing the behavior values calculated through the selected optimal technique with the actual behavior values.

Figure 4. The linear stage and example of block behavior detection experiment

3.2 Structure behavior detection experiment

Fig. 5 shows example of structure behavior detection experiment. The behavior was analyzed by taking images before and after the horizontal displacement, vertical displacement, and combined displacement of 12 parts distributed in the structure image. By applying the optimal feature detector and descriptor selected through the block behavior detection experiment, the value was calculated based on the position before and after the behavior $(\Delta d_{xi}, \Delta d_{yi})$ of the object in the structure, and it was verified by comparing the measured value using the total station.



Figure 5. The example of structure behavior detection experiment

4 RESULT AND DISCUSSION

4.1 Block behavior detection experiment

Fig. 6 shows distribution of repeatability with different feature matching techniques at each displacement type. Repeatability represents the efficiency of feature matching as the ratio of the number of feature extraction points in the target area before the behavior occurs in image pairs and the number of matching points used when performing feature matching. In all behavioral types, KAZE and SURF techniques showed high repeatability,

and θ_x was small at 5 ° and 85 °, which are the closest to 0° and 90°. Small repeatability means fewer matching points compared to features. As θ_x approaches 0° and 90°, the features in the image are similarly extracted, but each feature changes significantly as the behavior occurs. Therefore, matching is not performed for features that have changed significantly according to the occurrence of the behavior, and matching efficiency decreases as it approaches 0° and 90°.

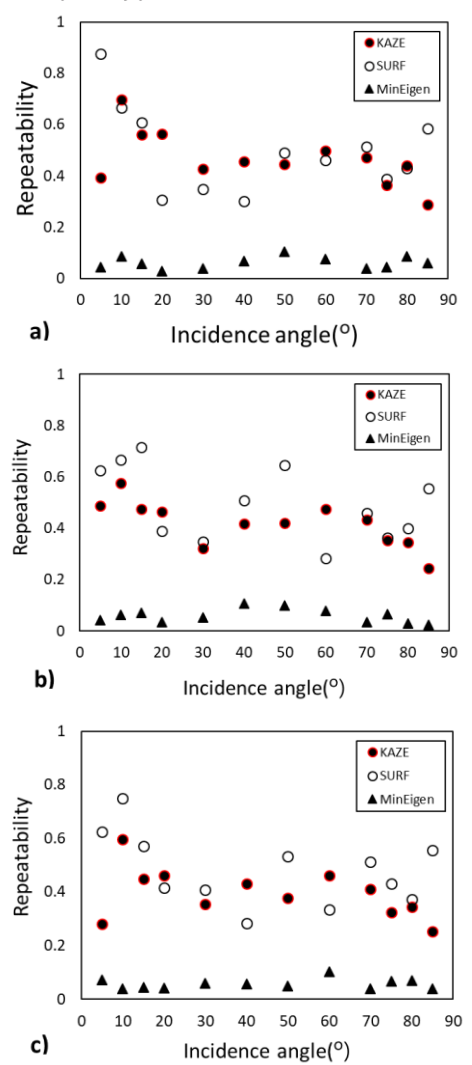


Figure 6. Distribution of repeatability with different feature matching techniques at (a) horizontal displacement, (b) vertical displacement and (c) combined displacement.

Fig. 7 shows distribution of BRE with different feature matching techniques at each displacement type. The BRE was calculated based on the registration error of the upper, lower, left, and right axes of the block, and is the basis for calculating the accuracy of feature matching based on the location of matching features. Regardless of the behavior type, the KAZE technique showed the least BRE, and registration through feature matching was performed with high accuracy. The KAZE technique shows the highest accuracy in repeatability and BRE. The KAZE technique showed that the feature extraction performance through the detector was 12.41 times compared to SURF and 2.56 times compared to MinEigen. The matching performance through descriptor was 11.33 times compared to SURF and 20.5 times compared to MinEigen. The KAZE technique, which includes a high-performance detector and descriptor, was selected as the optimal feature matching technique according to the block shape and behavior. As for the error of the behavior result measured by

the KAZE technique, the measured error was 0.29mm for the 30° - 60° section where the error stably appears.

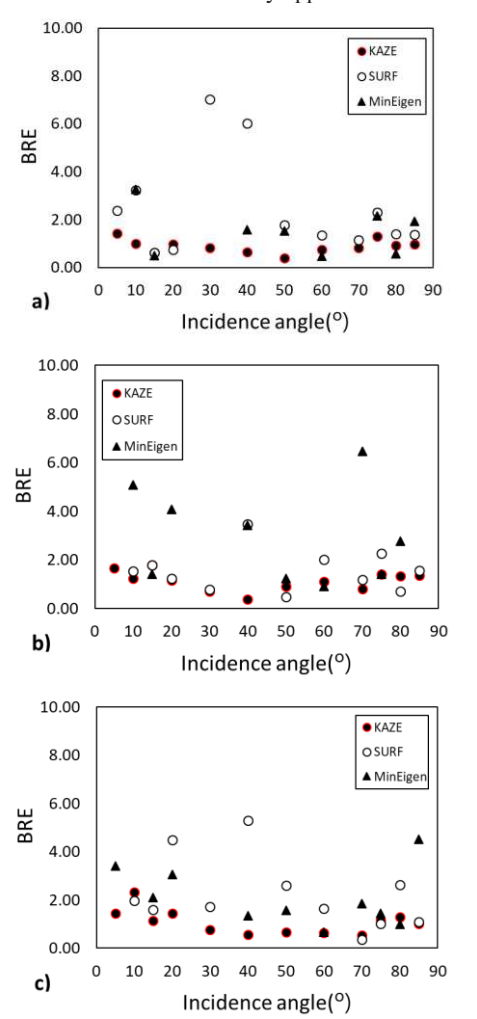


Figure 7. Distribution of BRE with different feature matching techniques at (a) horizontal displacement, (b) vertical displacement and (c) combined displacement.

4.2 Structure behavior detection experiment

Fig. 8 shows experimental results using the single camera system at each displacement type. The blue square represents the shape of the structure before behavior occurs, the black square represents the shape of the structure measured through the total station, and the red square represents the shape of the structure calculated through the single camera system. The average of the behavior values measured through the total station is horizontal displacement (dh: 64.41mm, dv: -2mm), vertical displacement (dh: -4.16mm, dv: -63.75mm), combined displacement (dh: 56.94mm, dv: -2mm), respectively. dv: -64.16mm), and the behavior values measured through a single camera system were horizontal displacement (dh: 66.35mm, dv: -3.2mm), vertical displacement (dh: -7.26mm, dv: -65.77), respectively. mm), combined displacement (dh: 54.94mm, dv: -66.18mm). The errors that occurred in each behavior type were 3.04% (horizontal displacement), 3.18% (vertical displacement), and 3.34% (combined displacement), showing excellent results.

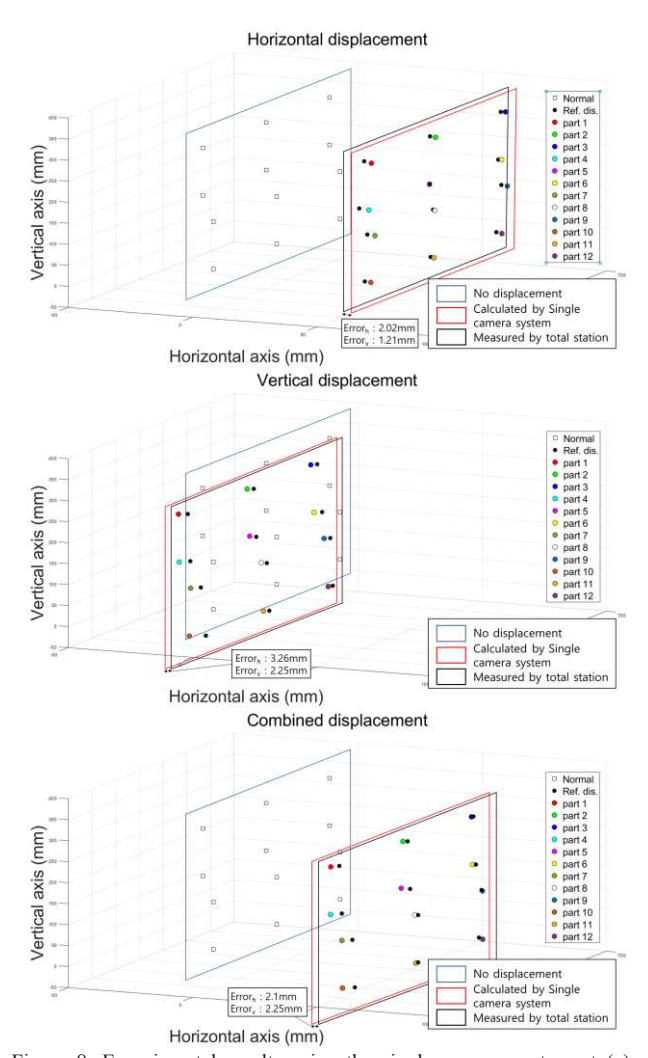


Figure 8. Experimental results using the single camera system at (a) horizontal displacement, (b) vertical displacement and (c) combined displacement.

5 CONCLUSIONS

This study aimed to develop a technique to analyze the behavior of MSEW structures based on images taken from a single viewpoint. It has economical excellence because it analyzes through images taken from a single viewpoint. Two types of experiments were conducted to develop and verify the single camera system, the main findings of this study include:

- The displacement in the lateral direction does not occur depending on the structural conditions of the retaining wall structure. The actual behavior of the retaining wall was also measured in images taken from a single point of view. The distance between the camera and the structure (D_r) , the angle in the x direction of the camera and the structure (θ_x) and camera parameters were used to calculate the actual behavior of blocks and structures based on Δd_{xi} and Δd_{yi} in the image
- A feature matching technique was applied to continuously extract the same target block as the behavior occurred. KAZE detector and descriptor showed excellent results in repeatability and BRE in detecting block-type behavior. Compared to other techniques, the detector showed up to 12.41 times and the descriptor up to 20.5 times, so it was selected and used as the optimal technique for block and behavior.

 The behavior calculated through the single camera system and the error calculated through the actual behavior were averaged 2.9% in the block test and 3.19% in the structure test, and showed excellent results as a vision-based monitoring technology.

In the future, real-time image analysis technology and noise (focus and camera shake, etc.) correction techniques will be developed and used more widely.

5 ACKNOWLEDGEMENTS

This work is supported by the Korea Agency for Infrastructure Technology Advancement(KAIA) grant funded by the Ministry of Land, Infrastructure and Transport (Grant 21TSRD-B151228-03).

6 REFERENCES

- Aldosari, M., Al-Rawabdeh, A., Bullock, D., and Habib, A. 2020. A mobile LiDAR for monitoring mechanically stabilized earth walls with textured precast concrete panels. Remote Sensing, 12(2), 306. doi:10.3390/rs12020306
- Bathurst, R.J., and Benjamin, D.J. 1990. Failure of a geogrid-reinforced soil wall. Transportation Research Record, 1288, 109-116.
- Benjamim, C.V.S., Bueno, B.S., and Zornberg, J.G. 2007. Field monitoring evaluation of geotextile-reinforced soil-retaining walls. Geosynth. Int., 14(2), 100-118.
- Choi, H.S., Cheung, J.H., Kim, S.H., and Ahn, J.H. 2011. Structural dynamic displacement vision system using digital image processing. NDT&E Int., 44(7), 597-608.
- Esmaeili, F., Varshosaz, M., and Saadatseresht, M. 2013. Displacement measurement of soil nail walls using close range photogrammetry. Procedia Engineering, 54, 516-524.
- Feng, D., Feng, M.Q., Ozer, E., and Fukuda, Y. 2015. A vision-based sensor for noncontact structural displacement measurement. Sensors, Vol. 15(7), 16557-16575.
- Fukuda, Y., Feng, M.Q., Narita, Y., Kaneko, S., and Tanaka, T. 2013. Vision-based displacement sensor for monitoring dynamic response using robust object search algorithm. IEEE Sensors Journal, 13(12), 4725-4732.
- Jiang, R., and Jauregui, D.V. 2010. Development of a digital close-range photogrammetric bridge deflection measurement system. Measurement, 43(10), 1431-1438.
- Koseki, J., and Hayano, K. 2000 Preliminary report on damage to retaining walls caused by the 1999 Chi-Chi earthquake. Bulletin of Earth Reinforcement Structure, University of Tokyo, 33, 23-34.
- Lee, J.J., and Shinozuka, M. 2006. Real-time displacement measurement of a flexible bridge using digital image processing techniques. Exp. Mech., 46(1), 105-114.
- Leonards, G.A., Frost, J.D., and Bray, J.D. 1994. Collapse of geogridreinforced retaining structure. Journal of Performance of Constructed Facilities, 8(4), 274-292.
- Oats, R.C., Escobar-Wolf, R., and Oommen, T. 2017. A novel application of photogrammetry for retaining wall assessment. Infrastructures, 2(3), 10. doi:10.3390/infrastructures2030010
- Oskouie, P., Becerik-Gerber, B., and Soibelman, L. 2016. Automated measurement of highway retaining wall displacements using terrestrial laser scanners. Automation in Construction, 65, 86-101.
- Panah, A.K., Yazdi, M., and Ghalandarzadeh, A. 2015. Shaking table tests on soil retaining walls reinforced by polymeric strips. Geotextiles and Geomembranes, 43(2), 148-161.
- Shinde, A.L., and Mandal, J.N. 2007. Behavior of reinforced soil retaining wall with limited fill zone parameter. Geotech. Geol. Eng., 25, 657-672.
- Yang, G., Zhang, B., Lv, P., and Zhou, Q. 2009. Behavior of geogrid reinforced soil retaining wall with concrete-rigid facing. Geotextiles and Geomembranes, 27(5), 350-356.
- Zhao, S., Kang, F., and Li, J. 2018. Displacement monitoring for slope stability evaluation based on binocular vision systems. Optik, 171, 658-671.